

High-quality processing of CFRP with a 1.1-kW picosecond laser

Christian Freitag^{1,2} · Margit Wiedenmann² · Jan-Philipp Negel² · André Loescher² · Volkher Onuseit² · Rudolf Weber² · Marwan Abdou Ahmed² · Thomas Graf²

Received: 17 February 2015 / Accepted: 31 March 2015 / Published online: 10 April 2015
© Springer-Verlag Berlin Heidelberg 2015

Abstract Carbon fiber-reinforced plastic (CFRP) was processed with a unique ultrafast laser delivering 8-ps pulses and an average output power of up to 1.1 kW at a pulse repetition rate of 300 kHz corresponding to a maximum pulse energy of about 3.7 mJ. Heat accumulation effects become the major issue at such high average powers. In the presented work, heat accumulation resulting from pulse overlap and from repetitive scans was investigated. The results allow estimating both the feed rates necessary to avoid heat accumulation by consecutive pulses and the maximum number of scans allowed avoiding detrimental heat accumulation by the consecutive scans in order to maintain good quality of the processed parts. The capabilities of the used laser source are being demonstrated cutting a contour out of 2-mm CFRP with an effective average cutting speed of 0.9 m/min and thermal damage smaller than 20 μm .

1 Introduction

Carbon fiber-reinforced plastics (CFRPs) are very inhomogeneous materials consisting of carbon fibers embedded in a polymer matrix. These two components exhibit a significant mismatch of their thermal properties [1–6], which can lead to thermal matrix damage during laser

processing. While the ablation process occurs in direction of the laser beam propagation, the thermal damage mainly spreads along the carbon fibers into the material due to their high heat conductivity. The growth of the matrix damage was observed in [7] by means of high-speed imaging. The heat-affected area, where the matrix material is vaporized leaving blank carbon fibers, is called matrix evaporation zone (MEZ). The model described in [8] allows estimating the minimum possible extent of the damage in CFRP caused during laser processing. According to the model, the absorbed intensity has to exceed 10^8 W/cm^2 to ensure that the extent of the thermal damage caused by heat conduction along the carbon fibers is less than 10 μm . Such high intensities are conveniently achieved with ultrashort-pulsed lasers. However, even when using ultrashort pulses, the formation of thermal damage can still be observed in many cases [7]. This matrix damage is a consequence of the heat accumulation effect between consecutive laser pulses, referred to as pulse accumulation in the following. The pulse accumulation effect is known to be one main cause for thermal damage when processing CFRP with pulsed lasers. An analytical approximation describing heat accumulation was presented in [9, 10], where expressions are given for the increase in the temperature over time as a function of the material properties, the total number of pulses N_{Pulses} incident at one point on the work piece, the repetition rate and the pulse energy. Each laser pulse contributes to the heating of the processed material. The heat accumulates if the temporal delay between the pulses is not long enough to allow the cooling of the material to almost its initial temperature. A second heat accumulation effect is caused due to consecutive scans when using a multi-pass ablation processing strategy. This heat accumulation effect is referred to as scan accumulation in the following. In this

✉ Christian Freitag
christian.freitag@ifsw.uni-stuttgart.de

¹ Graduate School of Excellence Advanced Manufacturing Engineering GSaME, Universität Stuttgart, Nobelstraße 12, 70569 Stuttgart, Germany

² Institut für Strahlwerkzeuge IFSW, Universität Stuttgart, Pfaffenwaldring 43, 70569 Stuttgart, Germany

case, the number of energy inputs is given by the applied number of scans over the material, and the temporal delay between the energy inputs is given by the temporal interval between consecutive scans at one location. The impact of this effect was demonstrated in [11] for a continuous wave laser system at a wavelength of 1068 nm. It was shown that there is a strong increase in the thermal damage if the temporal interval Δt_{Scans} between consecutive scans was too short. Heat accumulation results in both cases in additional thermal damage of the material.

where f_{Scans} is the repetition rate of the consecutive scans, t_{Scan} is the processing time of a given contour of the length l_{contour} , t_{Pos} is the positioning time, v_{Pos} is the positioning speed of the scanner system, l_{Pos} is the length of the positioning trajectory, and t_{pause} is a temporal pause between consecutive scans, e.g., for processing another part.

For a certain feed rate, material thickness d , kerf width b and average laser power P_{av} , the minimum number of scans N_{min} of the laser beam over the material which is required to cut the material can be estimated by energetic considerations and is given by

$$N_{\text{min}} = \frac{[r_{\text{fiber}} \cdot (E_{\text{heat,fiber}} + E_{\text{sub,fiber}}) + r_{\text{matrix}} (E_{\text{heat,matrix}} + E_{\text{sub,matrix}})] \cdot v_{\text{feed}} \cdot b \cdot d}{\eta_A \cdot P_{\text{av}}}, \quad (4)$$

1.1 Parameters defining the heat accumulation effects

The accumulation of heat depends on the number of energy inputs into the material and the temporal delay between these events. For the pulse accumulation effect, the temporal delay between two energy inputs equals the temporal delay Δt_{Pulses} between consecutive pulses and is given by

$$\Delta t_{\text{Pulses}} = \frac{1}{f_{\text{Pulses}}}, \quad (1)$$

where f_{Pulses} is the pulse repetition rate of the laser. When the laser beam is moved over the work piece surface at a velocity v_{feed} during the process, the number of energy inputs is given by the number of pulses at one location. This number assuming a top-hat intensity profile is given by

$$N_{\text{Pulses}} = \frac{d_f \cdot f_{\text{Pulses}}}{v_{\text{feed}}}, \quad (2)$$

where d_f is the diameter of the focal spot on the work piece. To minimize the pulse accumulation, a low value of N_{Pulses} is favorable. As the temperature monotonously increases with N_{Pulses} [10], it is seen from Eqs. (1) and (2) that a low pulse repetition rate and a high feed rate and a small focal spot reduce the pulse accumulation effect.

For the scan accumulation effect, the temporal delay between two energy inputs corresponds to the temporal delay Δt_{Scans} between two consecutive scans and is given by

$$\begin{aligned} \Delta t_{\text{Scans}} &= \frac{1}{f_{\text{Scans}}} = t_{\text{Scan}} + t_{\text{Pos}} + t_{\text{pause}} \\ &= \frac{l_{\text{contour}}}{v_{\text{feed}}} + \frac{l_{\text{Pos}}}{v_{\text{Pos}}} + t_{\text{pause}}, \end{aligned} \quad (3)$$

where $E_{\text{heat,fiber}}$ and $E_{\text{heat,matrix}}$ are the energy required to heat a volume of carbon fibers and the matrix material up to their evaporation temperature, respectively. Accordingly, $E_{\text{sub,fiber}}$ and $E_{\text{sub,matrix}}$ are the energies needed to overcome the latent heat of carbon fibers and the matrix material, respectively. The factors r_{fiber} and r_{matrix} denote the fraction of carbon fibers and matrix material in the compound, respectively. η_A is the absorptivity of CFRP taking into account multiple reflections between the carbon fibers. Calculated values for the absorptivity of CFRP based on a ray tracing model can be found in [12]. Due to loss mechanisms such as heat conduction and overheating of the material, the number of scans N_{Scans} actually needed in practice is larger than N_{min} and is given by

$$N_{\text{Scans}} = \frac{1}{\eta_P} \cdot N_{\text{min}}, \quad (5)$$

where η_P is the process efficiency.

1.2 Laser cutting of CFRP

In the literature, laser cutting of CFRP was investigated with both continuous wave and pulsed laser systems. Using a ns-laser system with an average laser power of 23 W, drilling of 2.5-mm-thick CFRP with an effective cutting speed of 0.016 m/min and an extent of the thermal damage well below 10 μm was shown in [13]. Increasing the average laser power significantly to 403 W at pulse durations of about 7 ps, cutting of 2-mm-thick CFRP with an effective cutting speed of 0.3 m/min was demonstrated in [14]. In this case, a heat-affected zone of 250 μm was observed [14]. Using a cw laser system with 1 kW average laser power, cutting of 2.4-mm-thick CFRP with cutting speeds of up to 3.5 m/min was achieved but again with the

disadvantage of a heat-affected zone of about 100–150 μm [15].

With the ongoing progress of the available short-pulse laser sources regarding increase in available average power, the investigations into heat accumulation become even more important to decide on adequate process strategies. In the following, we therefore report on experimental investigations of the heat accumulation effects in CFRP using a recently developed multi-pass thin-disk laser amplifier providing an average output power of up to 1.1 kW at a pulse duration of 8 ps [16].

2 Experimental setup

The maximum average output power of the laser used for this study was 1.1 kW at a constant pulse repetition rate of 300 kHz corresponding to a maximum pulse energy of 3.7 mJ. The laser emits at a wavelength of 1030 nm with a beam quality factor $M^2 < 1.4$. The duration of the pulses was about 8 ps.

A fast scanner system was used in combination with an F-Theta focusing lens with a focal length of 340 mm, which gave a maximum feed rate of the laser beam of 30 m/s on the CFRP surface of the samples. The beam had a diameter of approximately 5 mm on the focusing lens, which resulted in a focal diameter of about 125 μm (at $1/e^2$ intensity level). The Rayleigh length was calculated to be about 8.5 mm. With the above pulse energy and pulse duration, the incident intensity is $7.5 \times 10^{12} \text{ W/cm}^2$, and the fluence on the work piece amounts to 60 J/cm^2 .

The CFRP samples used were Toray T700S-12k carbon fibers with a RTM 6 matrix, which is a monocomponent resin. The carbon fibers were arranged in different layers with the orientation [0/90, -45/+45, 90/0, 0/90, -45/+45, 90/0]. The volume fraction of carbon fibers in the CFRP was 50 %.

The samples were processed by ablating on a circular path with a diameter of 50 mm, which gives a contour length $l_{\text{contour}} = 157 \text{ mm}$ in a multi-pass process. With this contour, the temporal interval Δt_{Scans} between consecutive scans only depends on the feed rate since the contour

length is constant. No pause was implemented, and no positioning time is necessary, see Eq. (3). The average laser power, the feed rate of the laser beam and its number of scans over the work piece were varied for the experiments. The processed samples were cut and polished to obtain cross sections of the ablated grooves. Two cross sections per sample were analyzed with an optical microscope to measure the thermal damage for each set of processing parameters.

A series of cross sections of samples ablated with 1.1 kW of average power and a feed rate of 30 m/s is shown in Fig. 1a–c. Within this series, the number of scans of the laser beam over the work piece was increased from 50 to 200. The MEZ can clearly be distinguished from the unaffected CFRP. It was only measured in layers where the carbon fibers are oriented perpendicular to the groove as this is the region with the largest extent of the heat-affected zone (due to the large heat conduction along the fiber axis). If the first layer of carbon fibers was not completely penetrated as shown in Fig. 1a, b, the MEZ was only measured at the top 50 % of the groove. The matrix layer at the surface of the sample was excluded from the measurement. Multiple values of the MEZ were measured on the left and right side of each groove as shown in Fig. 1a–c as red dotted lines, and the values were averaged.

3 Experimental results for different feed rates

3.1 Pulse accumulation

The pulse accumulation effect was investigated at different feed rates by applying only 15 consecutive scans of the laser beam over the same trajectory. For this number of scans, the influence of the scan accumulation effect can be neglected at $v_{\text{feed}} > 3 \text{ m/s}$ as seen from the data presented in the following. The maximum feed rate used was 30 m/s while the minimum feed rate without an observable influence of scan accumulation was 4.3 m/s. For $v_{\text{feed}} = 30 \text{ m/s}$, the applied number of pulses is only about 1.25 and about 8.71 for $v_{\text{feed}} = 4.3 \text{ m/s}$.

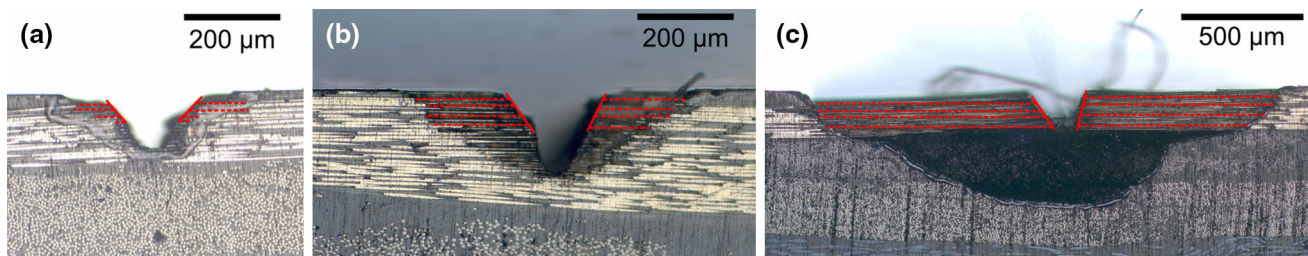


Fig. 1 Examples of polished cross sections of CFRP samples ablated with an average laser power of 1.1 kW and a feed rate of the laser beam of 30 m/s showing the resulting groove after **a** 50 scans, **b** 100 scans and **c** 200 scans

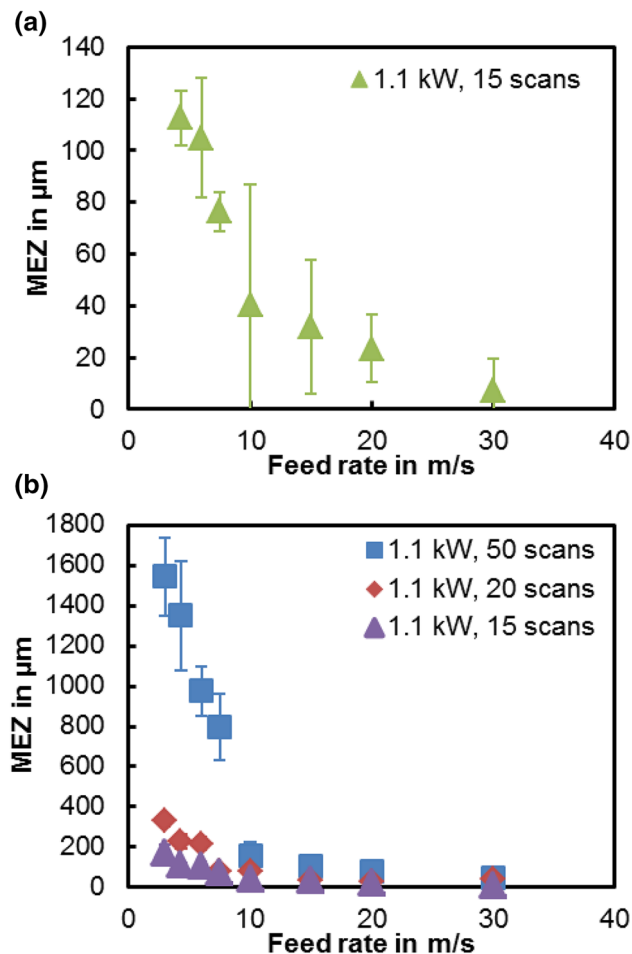


Fig. 2 **a** The MEZ as a function of the feed rate for 1.1 kW average laser power and 15 consecutive scans over the same trajectory. **b** The MEZ as a function of the feed rate for 1.1 kW average laser power and 15 (triangles), 20 (diamonds) and 50 (squares) scans over the same trajectory

Figure 2a shows the MEZ resulting after 15 consecutive scans when ablating CFRP with an average laser output power of 1.1 kW with different feed rates. At the maximum feed rate of 30 m/s, the lateral extent of the MEZ is less than 10 μm, while at a feed rate of 4.3 m/s, the extent of the MEZ reaches about 110 μm.

It can be seen in Fig. 2a that a decrease in the feed rate from 30 to 20 m/s and therefore an increase in the applied number of pulses N_{pulses} from 1.25 to 1.87 already cause an increase in the MEZ. As shown in [10], each laser pulse contributes to the cumulative heating of the processed material gradually increasing the temperature of the surrounding material. The extent of the MEZ is given by the region where the resulting temperature exceeds the evaporation temperature of the matrix material. To limit the influence of the pulse accumulation effect, the number of pulses applied at one spot should be reduced by choosing a high feed rate up to complete separation of the consecutive laser pulses.

3.2 Scan accumulation

In addition to the pulse accumulation effect, the above-mentioned scan accumulation also contributes to the increase in the temperatures but on a slower time scale. The influence of the scan accumulation effect on the extent of the MEZ can be seen from Fig. 2b where the MEZ is shown as a function of the feed rate for 1.1 kW average laser power and a number of 15 (triangles), 20 (diamonds) and 50 (squares) scans over the same trajectory. It is noted that the scale of the ordinate changes from Fig. 2a, b. For the circular shapes ablated with 20 scans, an increase in the MEZ for feed rates of ≤ 6 m/s can be seen compared to the circular shapes ablated with 15 scans. For $v_{\text{feed}} = 6$ m/s, the MEZ increases from about 110 μm for $N_{\text{Scans}} = 15$ –220 μm for $N_{\text{Scans}} = 20$. With an increasing number of scans, the feed rate below which the scan accumulation effect can be observed also increases. For $N_{\text{Scans}} = 50$, additional thermal damage due to scan accumulation can already be seen for $v_{\text{feed}} \leq 20$ m/s. For $v_{\text{feed}} = 20$ m/s, the MEZ was measured to be approximately 80 μm for $N_{\text{Scans}} = 50$, whereas for $N_{\text{Scans}} \leq 20$, the extent of the MEZ is only about 30 μm.

As a consequence of the scan accumulation effect, the matrix material starts to burn, which leads to an abrupt increase in the extent of the MEZ. This increase due to burning can be seen in Fig. 2b from the data corresponding to 50 scans between $v_{\text{feed}} = 10$ and 7.5 m/s.

The extent of the MEZ as a function of the number of scans is shown in Fig. 3a for $v_{\text{feed}} = 20$ and 30 m/s. The dotted lines are included to facilitate data interpretation. For a certain number of scans, the width of the MEZ is about 40 μm for both feed rates and does not increase with an increasing number of scans. This indicates that in this regime the matrix damage is only caused by pulse accumulation or by single-shot damage. At a critical number of scans, i.e., $N_{\text{S,crit},20\text{m/s}} \cong 35$ and $N_{\text{S,crit},30\text{m/s}} \cong 62$, the beginning of a strong increase in the MEZ can be seen for a feed rate of 20 and 30 m/s, respectively. This critical number of scans qualitatively indicates the onset of the scan accumulation effect causing additional matrix damage. $N_{\text{S,crit}}$ is a characteristic parameter for the scan accumulation effect and is very important to be considered for high-quality processing.

This critical number of scans $N_{\text{S,crit}}$ is shown as a function of the feed rate in Fig. 3b for an average laser power of 1.1 kW. The values $N_{\text{S,crit}}$ in this graph were determined as the average of the numbers of scans directly before and after a first enlargement of the MEZ was observed with increasing numbers of scans. The error bars indicate these two values. It is seen that the critical number of scans decreases with decreasing feed rates. Therefore, high feed rates are not only favorable regarding the pulse

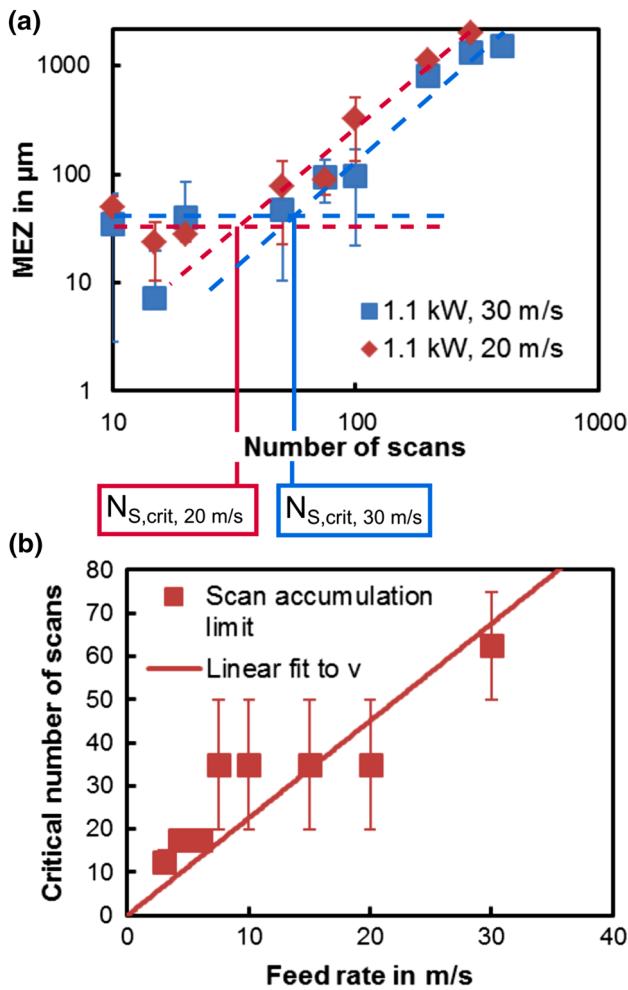


Fig. 3 **a** The extent of the MEZ as a function of the number of scans over the same trajectory for 1.1 kW of average laser power and feed rates of 20 and 30 m/s. Lines are included to guide the eye. **b** The critical number of scans as a function of the feed rate for 1.1 kW of average laser power. The line is a linear fit to the data points

accumulation effect but also regarding scan accumulation. The feed rate influences the temporal delay between two consecutive scans, see Eq. (3), as well as the energy input per scan, see Eq. (2). The function $N_{S,crit}(v) = av$ was fitted to the data points with a as the free parameter. The resulting line shows a reasonable agreement to the data points. The fit indicates a linear correlation between the feed rate and the critical number of scans.

4 Experimental results for different average laser powers

The influence of different average laser powers was investigated at a constant feed rate of 30 m/s for different numbers of scans. The average laser power directly

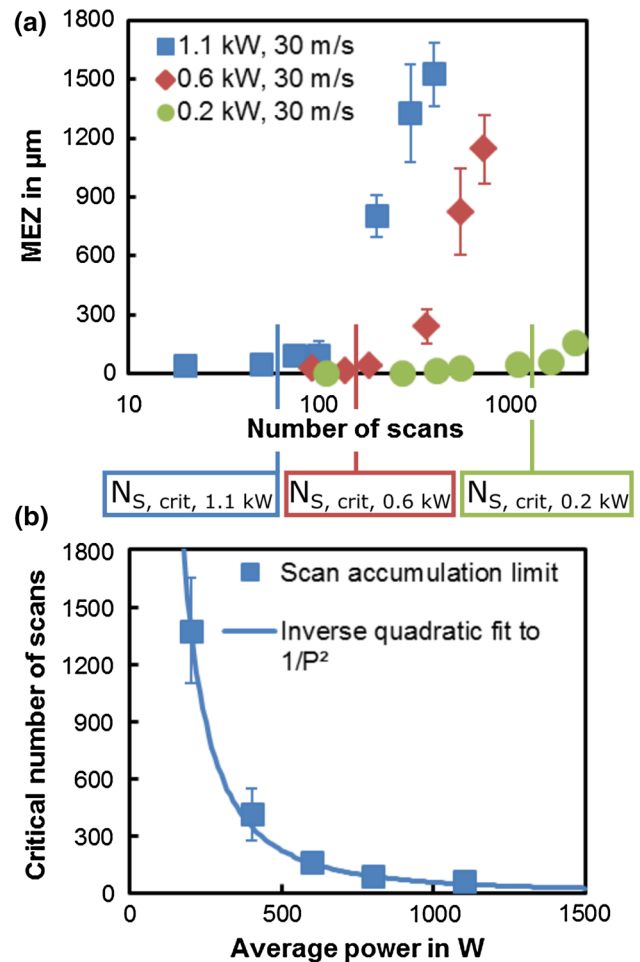


Fig. 4 **a** The extent of the MEZ as a function of the number of scans over the same trajectory is shown for three different average laser powers and a feed rate of 30 m/s. **b** The critical number of scans is shown as a function of the average laser power at a feed rate of 30 m/s. An inverse quadratic equation is fitted to the data points

influences the energy deposited as heat in the material per scan. However, the actual amount of energy that contributes to the heating of the material also depends on parameters such as the pulse energy [10] and the pulse repetition rate [17]. The measured MEZ as a function of the number of scans is shown in Fig. 4a. The different numbers of scans N_{Scans} were adapted with respect to the average laser power so that the total incident laser energy $E_{tot} = P_{av} \cdot N_{Scans} \cdot \Delta t_{Scans}$ remains constant for corresponding points. This ensures comparable depths of the ablated grooves for the different average laser powers. The temporal interval Δt_{Scans} between consecutive scans was 5.24 ms at all average laser powers since the ablated geometry and the feed rate were kept constant.

It is seen from Fig. 4a that after exceeding the critical number of scans the width of the MEZ increases for all

applied average laser powers with increasing number of scans. At a given number of scans, on the other hand, the maximum extent of the MEZ reached significantly increases with the increasing average laser power. For an average laser power of 200 W, the maximum extent of the MEZ at $N_{\text{Scans}} = 2200$ (about 12 s of processing time) is 160 μm , while for 1.1 kW, the MEZ reaches an extent of 1500 μm already at $N_{\text{Scans}} = 400$ (about 2 s of processing time). For lower average laser powers, less heat is deposited in the material during one scan. In combination with the longer overall processing time, the material has more time to cool down, which results in a smaller MEZ.

The influence of the average laser power on the critical number of scans for scan accumulation is shown in Fig. 4b. The critical number of scans increases for a decreasing average laser power. The function $N_{\text{S,crit}}(P_{\text{av}}) = b/P_{\text{av}}^2$ was fitted to the data points with b as the free parameter. The resulting line shows an excellent agreement to the data points. The fit indicates an inverse quadratic correlation between the average laser power and the critical number of scans.

The critical number of scans is a very important process-defining parameter when using a multi-pass ablation process. As shown in the experimental data presented in Figs. 3b and 4b for our given contour length of 157 mm, the critical number of scans is proportional to the feed rate divided by the average laser power squared,

$$N_{\text{S,crit}} \propto \frac{v_{\text{feed}}}{P_{\text{av}}^2}. \quad (6)$$

In this study, the contour length was kept constant, but it is also a defining parameter for the critical number of scans since the time between two consecutive scans depends on the contour length, see Eq. (3). The relation described in Eq. (6) has direct consequences for the process strategy: First, depending on average power and feed rate, the

volume of the ablated material in a given application defines the total number of scans required. To cut, e.g., a 2-mm-thick sample of CFRP with a feed rate of 30 m/s and a kerf width of 200 μm , a number of about 2100 scans are necessary with the laser used for our experiments. Equation (6) can be fulfilled either by reducing the average power of the laser or by introducing process pauses at every time when $N_{\text{S,crit}}$ is reached. It is noted that P_{av} is the average power applied to one processed contour; hence, simultaneous parallel processing of several contours is a suitable strategy to take benefit of lasers with high average powers.

5 Cutting of CFRP with high quality and high productivity

The above findings were applied to demonstrate high-quality processing at high average powers. A rectangular-shaped CFRP part was cut with 1.1 kW of average laser power (with 8 ps of pulse duration and 300 kHz of repetition rate). According to Eq. (3), a high feed rate of 30 m/s and a contour length of 630 mm were chosen to increase the temporal delay between two consecutive scans to 21 ms. However, this is not long enough to completely avoid scan accumulation. Therefore, after every 200 scans, a pause of about 1 min was implemented. The duration of this pause was not yet optimized and is certainly much too long. On the other hand, the pauses can be used for other processes to further improve the productivity.

A view on the cut part from the top is shown in Fig. 5a. It is noted that the gap seen in the photograph between the cut parts does not represent the actual ablated kerf width. The minimum number of scans for cutting of the material can be calculated according to Eq. (4) to be $N_{\text{min}} = 590$. In total, about 2100 scans were necessary to completely cut

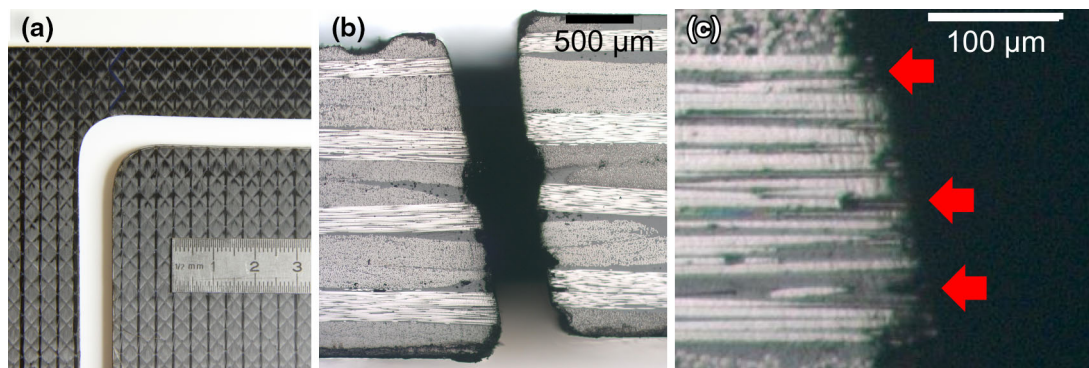


Fig. 5 Photograph of the CFRP part cut with an average laser power of 1.1 kW, a feed rate of 30 m/s and an effective average cutting speed of 0.9 m/min. **a** Top view of the cut. **b** Microscope image of a cross section of the cut. The width of the gap does not represent the

actual cutting kerf. **c** Magnified microscope image of the left, inner part of the cut. CFRP has been cut with a thermal damage smaller than 20 μm . The damaged areas are indicated by red arrows

the material. This gives a process efficiency of $\eta_p = 28\%$ according to Eq. (5). With the applied feed rate of 30 m/s and not taking the pauses into account, the effective average cutting speed was 0.9 m/min.

A cross section of the cut can be seen in Fig. 5b. The inner part of the cut rectangle can be seen on the left side, while the outer part is shown on the right. The gap between the two parts does again not represent the actual ablated kerf width. The kerf is inclined by about 11° , which results from the F-Theta focusing optics. Since the rectangle has a dimension of about $22.5\text{ cm} \times 9.5\text{ cm}$, cutting was mainly in the outer regions of the available scanning field where the laser beam is significantly inclined. The inclination of the kerf could be avoided by, e.g., using a telecentric focusing optics.

In the magnification of the cut in Fig. 5c, the areas of the cut with thermal damage of up to $20\text{ }\mu\text{m}$ are indicated by red arrows. Although no thermal damage is visible at a first glance, detailed inspection with the microscope reveals a few areas on the kerf surface where thermal damage was observed. Deviations of $80\text{ }\mu\text{m}$ in the straightness of the cut can be observed.

6 Summary

Ablation experiments of CFRP with an ultrafast laser system with an average laser power of up to 1.1 kW, a repetition rate of 300 kHz and a pulse duration of 8 ps were shown. The main issue when laser processing CFRP with such a laser system is heat accumulation effects. It was shown that higher feed rates and therefore smaller pulse overlaps decrease the influence of the pulse accumulation effect on the MEZ. A very important influencing factor on the MEZ formation when using a multi-pass process is the scan accumulation effect. This effect can lead to a burning of the matrix material and therefore to vast thermal damage. A characteristic value for the scan accumulation effect is the critical number of scans above which the extent of the MEZ starts to increase very rapidly. The dependence of the MEZ and the critical number of scans on the feed rate and the average laser power have been shown. The factors influencing the pulse and scan accumulation like the contour length and the temporal gap between consecutive scans were also discussed.

The capabilities of the used innovative laser source were demonstrate cutting a contour out of 2-mm CFRP with an effective average cutting speed of 0.9 m/min and thermal damage smaller than $20\text{ }\mu\text{m}$.

Acknowledgments This work was funded by the German Federal Ministry of Education and Research BMBF in the frame of the project

ProCaV under Contract No. 13N11911 and in the frame of the project T4nPV under Contract No. 13N11787 and the Graduate School of Excellence advanced Manufacturing Engineering GSaME of the University of Stuttgart.

References

1. C. Pradere, J.C. Batsale, J.M. Goyh n che, R. Pailler, S. Dilhaire, Thermal properties of carbon fibers at very high temperature. *Carbon* **47**, 737–743 (2009)
2. D.E. Kline, Thermal conductivity studies of polymers. *J. Polym. Sci.* **1**, 441–450 (1961)
3. B. Sundqvist, O. Sandberg, G. B ckstr m, The thermal properties of an epoxy resin at high pressure and temperature. *J. Phys. D Appl. Phys.* **10**, 1397–1403 (1977)
4. C.A. Griffs, R.A. Masumura, C.I. Chang, Thermal response of graphite epoxy composite subjected to rapid heating. *J. Compos. Mater.* **15**, 427–442 (1981)
5. G. Herzberg, K.F. Herzfeld, E. Teller, The heat of sublimation of graphite. *J. Phys. Chem.* **41**(2), 325–331 (1937)
6. T.A. Trigg, Carbon fibre composites in rocket motor systems. in *3rd British Interplanetary Society Symposium on Material in Space Technology, Bristol, England* (1969)
7. C. Freitag, V. Onuseit, R. Weber, T. Graf, High-speed observation of the heat flow in CFRP during laser processing. *Phys. Procedia* **39**, 171–178 (2012)
8. R. Weber, M. Hafner, A. Michalowski, T. Graf, Minimum damage in CFRP laser processing. *Phys. Procedia* **12**(2), 302–307 (2011)
9. R. Weber, C. Freitag, T.V. Kononenko, M. Hafner, V. Onuseit, P. Berger, T. Graf, Short-pulse laser processing of CFRP. *Phys. Procedia* **39**, 137–146 (2012)
10. R. Weber, T. Graf, P. Berger, V. Onuseit, M. Wiedenmann, C. Freitag, A. Feuer, Heat accumulation during pulsed laser materials processing. *Opt. Express* **22**(9), 11312–11324 (2014)
11. J. Stock, M.F. Zaeh, M. Conrad, Remote laser cutting of CFRP: improvements in the cut surface. *Phys. Procedia* **39**, 161–170 (2012)
12. C. Freitag, R. Weber, T. Graf, Polarization dependence of laser interaction with carbon fibers and CFRP. *Opt. Express* **22**(2), 1474–1479 (2014)
13. L. Romoli, F. Fischer, R. Kling, A study on UV laser drilling of PEEK reinforced with carbon fibers. *Opt. Lasers Eng.* **50**(3), 449–457 (2012)
14. J. Finger, M. Weinand, D. Wortmann, Investigations on processing of carbon fiber reinforced plastics using ultrashort pulsed laser radiation with high average power. in *Proceedings of the International Congress on Applications of Lasers and Electro-Optics (ICALEO)* (2013)
15. A. Klotzbach, M. Hauser, E. Beyer, Laser cutting of carbon fiber reinforced polymers using highly brilliant laser beam sources. *Phys. Procedia* **12**, 572–577 (2011)
16. J.-P. Negel, A. Voss, M.A. Ahmed, D. Bauer, D. Sutter, A. Killi, T. Graf, 1.1 kW average output power from a thin-disk multipass amplifier for ultrashort laser pulses. *Opt. Lett.* **38**(24), 5442–5445 (2013)
17. B. Neuenschwander, B. Jaeggi, M. Schmid, U. Hunziker, B. Luescher, C. Nocera, Processing of industrially relevant non-metals with laser pulses in the range between 10 ps and 50 ps. in *Proceedings of the International Congress on Applications of Lasers and Electro-Optics (ICALEO)* (2011)